Proceedings of 2022 IEEE
International Conference on Mechatronics and Automation
August 7 - 10, Guilin, China

The PG2 Gripper: an Underactuated Two-fingered Gripper for Planar Manipulation

Yonggan Yan[1], Shuxiang Guo[1*], Cheng Yang[1,2], Chuqiao Lyu[1], Liuqing Zhang[1]

[1] *Key Laboratory of Convergence Biomedical Engineering System and Healthcare Technology, The Ministry of Industry and Information Technology, Beijing Institute of Technology, Beijing, 100081, China*
[2] *School of Automation, Beijing Institute of Technology, Beijing, 100081, China*
E-mails: {guoshuxiang & yanyonggan}@bit.edu.cn;
*corresponding author

***Abstract*—The flexible grasping, twisting, and force sensing abilities of the gripper are theoretically significant and practically valuable to solve. However, it is still difficult for most existing grippers to realize these three functions simultaneously. In this paper, to realize the purposes of grasping, twisting, and sensing contact force, a novel parallel gripper the PG2 was developed. A two-finger grasping mechanism based on the parallelogram mechanism was designed and constructed. Meanwhile, to sense the contact force between the fingers and the object, a SEA-based force sensing mechanism was proposed. Then the relationship between the rotating angle of the object and the driver angle was calculated through kinematic analysis. Finally, a twisting platform was built and an evaluated experiment was carried out. The experimental results showed that the PG2 can grasp and twist the thin object with a high responding speed in the case of constant contact force. The novel mechanism for grasping, twisting, and sensing contact force has potential in the area that required high responding speed.**

***Index Terms*—Flexible grasping, grasping and twisting, force sensing, parallel gripper, underactuated gripper.**

I. Introduction

Grasping is one of the most crucial functions of robots, which is applied in end effectors. A simplified description of grasping is the ability to pick up and hold an object against external disturbances. Grasping is often realized by gripper in robotics, which consists of a set of mostly joints and links traditionally and is equipped with proprioceptive and exteroceptive sensors [1]. Although substantial achievements have been witnessed in robotic grasping during the past few decades [2], flexible grasping, adaptive grasping, and force sensing remain difficult [3]. Nevertheless, it is theoretically significant and practically valuable to solve the above three problems [4]. The importance of tactile sensing in human manipulation [5], as evidenced by decreased performance in individuals with a lack of tactile feedback has led to an interest in tactile sensing in the fields of robotics [6].

Since 2014, Yale university has launched a project named 'Yale OpenHand Project' [7], which is an initiative to advance the design and use of robotic hands designed and built through rapid-prototyping techniques to encourage more variation and innovation in mechanical hardware. Based on the project, Nicolas et al [8] proposed an underactuated two-fingered gripper "The GR2 Gripper", which can adapt objects with different sizes and shapes, such as the clamps shown in Fig. 1 (a). To realize the haptics of the gripper, Benjamin et al [9] proposed a tactile feedback component based on two TacTip sensors, as shown in Fig. 1 (b). Combining an active tactile perception algorithm, the GR2 gripper can reposition and reorient grasped objects. Although the above two grippers can perceive the position and shape of the subject, they can't perceive the grasping force, which is vital to avoid objects from damage. To this aim, Leif et al [10] proposed a miniature 'Takktile sensor' with the ability to sense grasping force based on MEMS barometers, which has great potential in using in stretchable or rigid curved surfaces. The Takktile sensors arrays are integrated into the i-HY hands for adjusting the force exerted on grasped objects, as shown in Fig. 1 (c) [11]. Obviously, to increase the arrays' resolution, high-density dots need to be set, which raise the complexity of the system and reduce the robustness. Tasbolat et al [12] proposed a two-fingered gripper equipped with dynamic tactile sensors, as shown in Fig. 1 (d). Combining machine learning models, the gripper can identify different food. However, the machine learning model, which is an offline prediction model, can't identify strange objects, so it limits the portability of the gripper.

The above studies show that the tactile gripper relies on the development of sensors. Besides, some grippers can measure the grasping force by modeling without sensors. Xu et al [4] designed an adaptive two-finger gripper based on the fin-ray structure, which enables an intrinsic force sensing ability without any tactile sensor, as shown in Fig. 1 (e). Although the large errors appear near its two ends, the modeling method has high adaptability. Structure modeling is famous for adaptability in soft robots. Based on elastic rod modeling, Vincent et al [13] illustrated the feasibility of the method to locate regions of high contact force along the

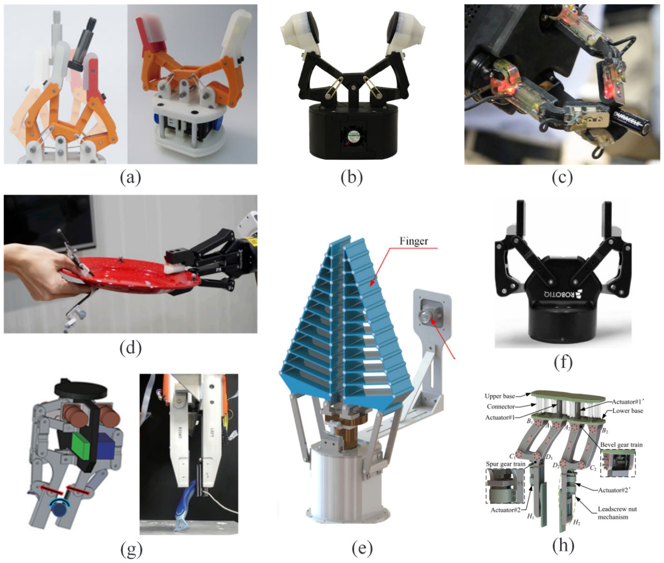

Fig. 1. Typical structures of current robotic grippers. (a) The GR2 Gripper. (b) The GR2 gripper with integrated TacTip sensors. (c) The i-HY Hand. (d) Gripper from National University of Singapore. (e) A compliant adaptive gripper from Harbin Institute of Technology. (f) Widely used clamps from ROBOTIQ. (g) The TP gripper. (h) four-DOF parallel gripper from Beijing University of Technology. [8].

rod. Xu et al [14] used screw theory to analyze the sensible wrenches and sense the force with low error. However, the study only allows force sensing in broad environments due to limitations such as size and MRI compatibility. Actually, the above hardware systems, which are robust by perceiving force through complex modeling based on material properties without any sensors, are fit for applications. Nevertheless, these existing methods have limitations. On the one hand, most of them are serious in material uniformity, which has a great impact on the model's accuracy. On the other hand, the deformation-force models of these robotic grippers, particularly in serious in the end or other parts, are usually nonlinear and complicated and bring many concerns on computation time and sensing accuracy.

The major objective of this research is to develop a gripper with simultaneous grasping, twisting and force sensing, especially in thin objects. To this aim, we design underactuated two-fingered gripper based on the parallelogram mechanism, investigate the coupling relationship between two motors, and realize force sensing and controlling. The gripper is inspired by the human index finger and thumb. Unlike other existing grippers [8]–[11], it can not only sense the force but also rotate subjects with desired grasping force between fingers. Finally, an experimental platform is built to verify the feasibility of the gripper.

II. Mechanical Design

In this section, a robotic gripper PG2 for grasping and twisting is designed to meet some requirements of the robot end. The architecture of the PG2 is shown in Fig. 2. The major design objectives are the parallel grasping mechanism and the force sensing ability.

A. PG2 Gripper Mechanical Design

Twisting is to grasp the objects with two or three human fingers and adjust its posture by moving the fingers in the same or opposite direction, which requires the collaboration of the thumb and the index finger. The traditional parallel grippers, which are inspired by human fingers, tend to rotate objects by controlling the relative motion of two fingers [15], [16]. A key to designing this gripper is how to ensure reliable twisting action without the object slipping off [16]. The reason why human fingers can twist operation stably is that the fingers contain complex tactile nerves, which enable people to actively adjust the clamping force of the object based on the manipulation, especially when the shape and weight of the clamping object are unknown.

To grasp and twist the objects, the PG2 gripper is designed based on the parallelogram mechanism. The mechanism has a simple and defining feature. The connecting line of two rotoidal joints in the base (the fixed link) is parallel to the connecting line of the coupler (the output link)' s. The mechanism is a single-DOF (degree of freedom) linkage mechanism, and its crank (the input link) can be driven to precisely control the position of the linkage in the motion space. But the motion space of any point on the coupler is the same as the rotoidal joints, which is an arc whose radius is the distance of the two joints in the crank. The traditional gripper using this mechanism tends to control the two parallelogram mechanisms to move toward each other based on the arc-shaped trajectory to realize the grasping of the object [17], as shown in Fig. 1 (f). But twisting the object, an important function for the gripper, requires adding an extra DOF. And the symmetrical and wide space occupation limits the application of this type of gripper.

The PG2 gripper contains three DOFs, including two active DOFs and one redundant DOF. Compared with the conventional gripper [15], [16], as shown in Fig. 1 (g) and Fig. 1 (h), the PG2 gripper only uses two servo motors (EC-max 16, Maxon, Switzerland) to grasp, release and twist objects. The PG2 are mainly composed of a redundancy finger and a reference finger with urethane pads (Shore hardness: 60A) attached to the working side. At the initial position of the compression spring, the joints of the two parallelogram mechanisms, which support the two fingers, are coaxial. The overlapping design of the gripper mechanism reduces the space occupation by almost 50%.

As shown in Fig. 2, the drive joint of the reference finger is fixed on the base, and the motion trajectory of each point

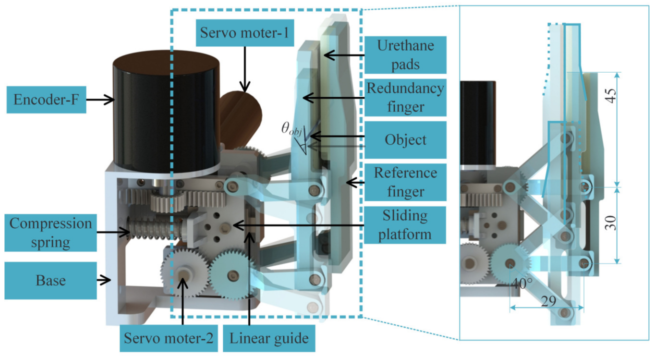

Fig. 2. Mechanical design of the PG2.

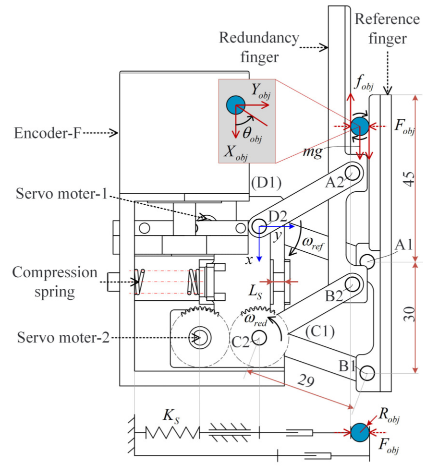

Fig. 3. Structural parameters of the PG2.

on the finger is a definite circular arc with a radius of 29mm. The drive joint of the redundancy finger is fixed on the sliding platform and moves with it. The drive joints of the two fingers are driven by servo motor-1 and servo motor-2, respectively. A sliding connection between the sliding platform and the base is formed by a linear guide, and the two parts fix one end of the compression spring in the sliding direction, respectively. The plane cartesian coordinate system is established by taking the reference finger drive joint as the center of the circle, the vector pointing to the another joint of the base is the X-axis, and it is rotated 90° counterclockwise as the Y-axis, as shown in Fig. 3. Along the Y-axis, a closed kinematic chain is formed by the base, the reference finger component, the object, the redundancy finger component, the sliding platform, and the compression spring. The pressure of the spring is equal to the grasping force of the object, which can be adjusted by controlling the component of the side link of the reference finger and the redundancy finger along the Y-axis. Then combined with the redundant DOF, the distance of the contact surfaces and the grasping force can be controlled accurately. The contact surfaces that are parallel to each other have the potential to hold thin objects, because the contact surfaces can be close to each other infinitely, in the case of the object with low bending stiffness or the center of gravity close to the grasping center.

The effective grasping range of the PG2 is the range within which the two contact surfaces can be opened when the redundant DOF are ineffective. As long as the maximum distance of the points on the cross-sectional envelope of the object is within this range, it can be grasped and twisted by the PG2, with the help of the redundant DOF. The gripper can hold objects within a size range of 15mm by adjusting the distance between the two fingers through two servo motors. The two fingers twist the object through relative parallel motion along the X-axis. The twist angle of the object is related to the length of the contact surfaces and the perimeter of the straight line family envelope of the gripping object. Simply, taking a cylinder as an example, the relationship between the twisting angle and the relative displacement of the two fingers can be expressed as:

$$\theta_{obj} = \frac{\Delta X}{2r_{obj}} \tag{1}$$

where ΔX represents the relative displacement of the two fingers along the X-axis, θ_{obj} represents the twisting angle of the cylinder, r_{obj} represents the radius of the cylinder.

B. PG2 Gripper Force Sensing

The traditional position control has been unable to satisfy the grasping of complex objects, and the object is easy to be slipped or damaged by the gripper due to excessive grasping force. Therefore, the design of the gripper with precise force feedback is imminent. Dimeas et al [18] installed multiple micro force sensors to the contact surface of the gripper, which are only used to measure the contact force of the contact surface during grasping and limited in twisting. The film pressure sensor can be attached to the gripper, which can directly obtain the contact force [19], [20]. However, the pressure sensor only measures the total pressure of the corresponding area, which is related to the contact state of the object, and has limitations in adjusting the object pose continuously.

The PG2 measures the contact force through a SEA (Series elastic actuator) whose elastic element is a compression spring, as shown in Fig. 3. The compression amount of the compression spring is converted into the rotation angle of an 11-bit encoder (RW-ARE-485-RTU-11-5-m-6, REAL-WETECH, China) through the rack and pinion transmission, and the precision is 0.01534mm after conversing to the compression amount. Assuming that the elastic coefficient of the compression spring is K_S, it generally has high stability due to material properties and mature manufacturing processes. Assuming that the compression amount of the

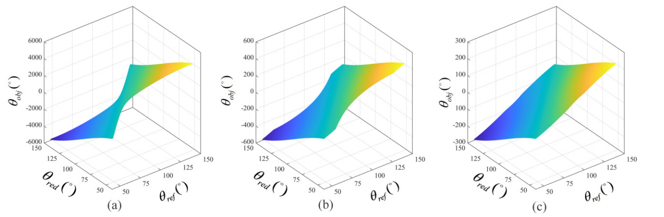

Fig. 4. Relationship between the rotating angle of the object with three radii and the two input links. (a) $R_{obj} = 0.25\text{mm}$. (b) $R_{obj} = 2.5\text{mm}$. (c) $R_{obj} = 5\text{mm}$.

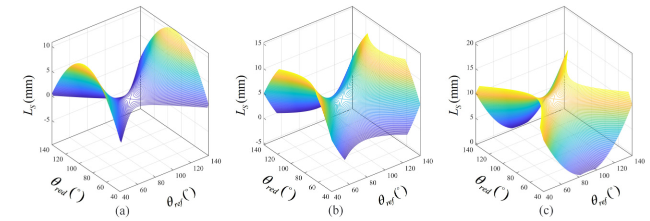

Fig. 5. Contour map of spring compression and crank joint angle. (a) $R_{obj} = 0.25\text{mm}$. (b) $R_{obj} = 2.5\text{mm}$. (c) $R_{obj} = 5\text{mm}$.

spring is L_S, it can be adjusted by controlling the component along the Y-axis of the two fingers in the closed kinematic chain. Then the grasping force of the object can be written as:

$$F_{obj} = K_S \cdot L_S \tag{2}$$

where F_{obj} represents the grasping force of the object. It should be noted that the gravity of the redundancy finger mechanism does not affect the amount of spring compression. Because the sliding direction is horizontal, gravity is converted into an internal force between the mechanism and the servo motor-2, so the spring pressure is strictly equal to the contact force.

C. PG2 Gripper Kinematics Analysis

In order to precisely control the posture of the object, an accurate kinematics solution is required. The purpose of this part is to obtain the analytical inverse solution of the motion space of the PG2 gripper and the position of the object, which is used to design the motion control algorithm. For simplicity, it is assumed that the cross section of the object is a perfect circle with a radius of R_{obj}, as shown in Fig.3. Meanwhile, it is assumed that the angle between the crank of the reference finger and the X-axis is θ_{ref} and the angle between the crank of the redundancy finger and the X-axis is θ_{red}. Taking $\theta_{ref} = 90°$, $\theta_{red} = 90°$ as the initial position, the abscissas of joints A1 and A2 are 0 in this state. The rotation angle of the gripping object can be expressed as:

$$\theta_{obj} = \frac{29(\cos\theta_{ref} - \cos\theta_{red})}{2R_{obj}} \cdot \frac{180°}{\pi} \tag{3}$$

The rotating angle of the object is related to its radius, which is set to 0.25mm, 2.5mm, and 5mm, respectively. Set the angle range of the input links of the two fingers to be $[40°, 140°]$. Without considering the mass of the object and the distribution of the center of gravity, the relationship between the rotating angle of the object with three radii and the two input links is calculated, as shown in Fig. 4.

The smaller the diameter of the object, the smaller the effective motion space, because the robot motion space where the distance between the two contact faces is larger than the diameter of the object is removed. In the removed part of the motion space, the two contact surfaces cannot contact the object at the same time, and when the reference finger drive-off angle is 90°, the effective motion space corresponding to the redundancy finger is the narrowest. The reason is that the displacement of the redundancy finger along the Y-axis cannot be greater than the diameter of the object to ensure that the compression spring has a certain force on it.

To twist the object under constant contact force, we need to control the rotation angle of the two fingers drivers collaboratively to ensure the constant deformation of the SEA elastic element. The amount of compression of the spring can be expressed as:

$$L_S = -29(sin\theta_{ref} - \sin\theta_{red} - 2R_{obj}) \tag{4}$$

Still take the above cylindrical objects with different diameters, and draw the contour map within the effective motion space with a resolution of 0.1mm of spring compression, as shown in Fig. 5.

The spring compression contours for the same object are symmetric about the planes $\theta_{ref} = 90°$ and $\theta_{red} = 90°$. When the gripper ensures a constant target contact force, the redundant DOF is cancelled, and the mechanism is converted into a grasping mechanism with two motion DOFs. On the premise that the contact surfaces are in close contact with the object, the motion space of the mechanism on the plane where the contour line is located has two symmetrical arcs, which are separated. One of the fingers cannot cover the motion space within its capability, that is, there is a dead zone, except that the spring compression is equal to the diameter of the object. It should be noted that the closer the spring compression is to the diameter of the object, the larger the motion space of the driver, and the larger the motion range of the corresponding object along the X-axis. In this paper, we only analyze the motion space of one side of the symmetry. Regarding the smooth transition of the dead zone of the separated motion space, we will make improvements in the future study to increase the twisting angle range.

Given the target contact force, that is, the amount of spring compression, we can inversely solve the two sets of the drivers' angle analytical expressions. The wire diameter of the spring used is 0.7mm, and the elastic coefficient is 1.47N/mm. Then on the premise that the kinematic chain is closed along the Y-axis, the two solutions of θ_{red} can be expressed as:

$$\theta_{red} = \frac{180}{\pi}\arcsin(\frac{100F_{obj}}{4263} - \frac{2R_{obj}}{29} + \sin(\frac{\pi}{180}\cdot\theta_{ref})) \tag{5}$$

$$\theta_{red}{}' = \frac{180}{\pi}(\pi - \arcsin(\frac{100F_{obj}}{4263} - \frac{2R_{obj}}{29} + \sin(\frac{\pi}{180}\cdot\theta_{ref}))) \tag{6}$$

Substitute (5) and (6) into (3) to obtain the rotating angle of the object, and θ_{obj} can be expressed as:

$$\theta_{obj} = -\frac{180}{\pi R_{obj}}(\frac{29}{2}\cos(\frac{\pi}{180}\cdot\theta_{ref}) \pm \frac{29}{2}(1 - (\frac{100F_{obj}}{4263} - \frac{2R_{obj}}{29} + \sin(\frac{\pi}{180}\cdot\theta_{ref}))^2)^{0.5}) \tag{7}$$

III. Evaluation and Experiments

In this section, an experiment was performed to evaluate the performance of the master-slave twisting angle tracking. Many researches have been done on the grasping and twisting of catheter and guidewire in vascular interventional surgery [21]–[26]. The twisting platform of the catheter is shown in Fig. 6. The platform includes the master side and the slave side, as shown in the red dashed box and the blue dashed box, respectively. On the master side, the encoder-M, which is an 11-bit encoder connected with a catheter, collected the twisting angle of the operator. On the slave side, a catheter with the encoder-S, which is an 11-bit encoder, was connected with the base for measuring the twisting accuracy of the PG2. Firstly, the gripper was initialized based on the limit position detection, as shown in Fig. 7. The reference finger was moved unidirectionally until the SEA detected contact with the stationary redundant finger and recorded the reference finger position as shown in Fig.7 (a) to (b). The reference finger was then moved in the opposite direction until the SEA again detected contact with the stationary redundant finger, and recorded the current reference finger position as shown in Fig. 7 (c). Then the angle between the redundant finger and the horizontal direction can be expressed as:

$$\theta_{redI} = \frac{\theta_{ref2} - \theta_{ref1}}{2} \tag{8}$$

where θ_{redI} represents the angle between the redundant finger and the horizontal direction, θ_{ref1} represents the angle of the first contact between the two fingers, θ_{ref2} represents the angle of the second contact between the two fingers. Then the two fingers moved in the same direction or opposite directions by an angle θ_{redI} to the desired initial state as shown in Fig. 7 (d), that is, their crank direction was the horizontal direction.

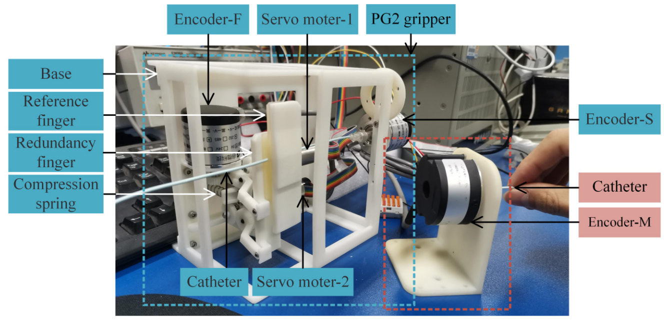

Fig. 6. Twisting platform of catheter.

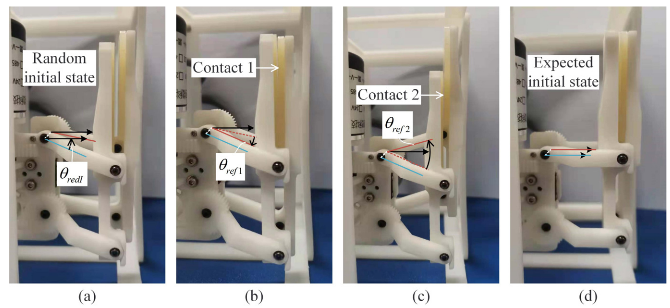

Fig. 7. Gripper position initialization based on limit position detection. (a) The random initial state. (b) The first contact. (c) The second contact. (d) The expected initial state.

In the twisting angle tracking experiment, to show the performance of the PG2 in responding speed and tracking accuracy, the operator was required to twist the catheter quickly and randomly. The measured master-slave twisting angle tracking curve is shown in Fig. 8.

As shown in the blue line of Fig. 8, the first twisting in the master side, which twisted 244.081°, was completed within 0.7s and another twisting, which twisted 234.360°, was 0.47s. The average twisting velocities of the two twistings were 348.687°/s and 498.638°/s, respectively. For the performance of the PG2, as shown in the red dashed line, the average twisting velocities of the two twistings were 591.46°/s and 444.6°/s, respectively. The static average error of the first twisting was 2.9296° and the relative static average tracking error was 1.216%. The static average error after the second twisting was 11.6868° and the relative static average tracking error was 2.443%. The master-slave postpone was 234ms.

IV. Results Analysis and Conclusion

In this article, a novel parallel gripper the PG2 was developed with the purposes of grasping, twisting, and sensing contact force. To this aim, a two-finger grasping mechanism based on the parallelogram mechanism was designed and

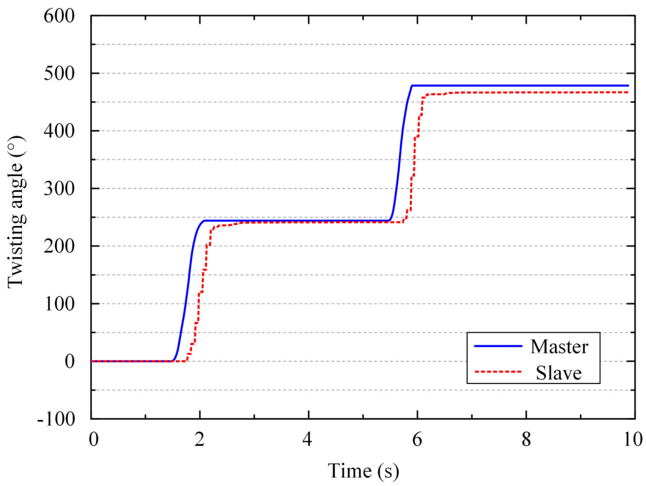

Fig. 8. Master-slave twisting angle tracking curve.

constructed. Meanwhile, to sense the contact force between the fingers and the object, a SEA-based force sensing mechanism was proposed. And then the kinematics analysis of the PG2 gripper was analyzed in the case of the constant contact force and the relationship between the rotating angle of the object and the driver angle was calculated. Finally, to evaluate the twisting performance of the PG2, a twisting platform for the catheter was built and an evaluated experiment was carried out. The experimental results showed that the static tracking error was existed due to the opened control system and the slipping of the catheter, but the relative static average tracking error was low and satisfied the requirement of operation. It should be noted that the PG2 gripper can twist the catheter with a high responding speed, which improves the efficiency of twisting. The novel mechanism for grasping, twisting, and sensing contact force has potential in the area that required high responding speed.

References

[1] B. Siciliano, O. Khatib, and T. Kröger, *Springer handbook of robotics*. Springer, 2008, vol. 200.

[2] U. Gupta, L. Qin, Y. Wang, H. Godaba, and J. Zhu, "Soft robots based on dielectric elastomer actuators: A review," *Smart Materials and Structures*, vol. 28, no. 10, p. 103002, 2019.

[3] J. Shintake, V. Cacucciolo, D. Floreano, and H. Shea, "Soft robotic grippers," *Advanced materials*, vol. 30, no. 29, p. 1707035, 2018.

[4] W. Xu, H. Zhang, H. Yuan, and B. Liang, "A compliant adaptive gripper and its intrinsic force sensing method," *IEEE Transactions on Robotics*, vol. 37, no. 5, pp. 1584–1603, 2021.

[5] R. S. Johansson and J. R. Flanagan, "Coding and use of tactile signals from the fingertips in object manipulation tasks," *Nature Reviews Neuroscience*, vol. 10, no. 5, pp. 345–359, 2009.

[6] H. Yousef, M. Boukallel, and K. Althoefer, "Tactile sensing for dexterous in-hand manipulation in robotics—a review," *Sensors and Actuators A: physical*, vol. 167, no. 2, pp. 171–187, 2011.

[7] GrabLab, "Yale openhand project," http://www.eng.yale.edu/grablab/openhand/, 2014.

[8] N. Rojas, R. R. Ma, and A. M. Dollar, "The gr2 gripper: An underactuated hand for open-loop in-hand planar manipulation," *IEEE Transactions on Robotics*, vol. 32, no. 3, pp. 763–770, 2016.

[9] B. Ward-Cherrier, N. Rojas, and N. F. Lepora, "Model-free precise in-hand manipulation with a 3d-printed tactile gripper," *IEEE Robotics and Automation Letters*, vol. 2, no. 4, pp. 2056–2063, 2017.

[10] L. P. Jentoft, Y. Tenzer, D. Vogt, J. Liu, R. J. Wood, and R. D. Howe, "Flexible, stretchable tactile arrays from mems barometers," in *2013 16th International Conference on Advanced Robotics (ICAR)*. IEEE, 2013, pp. 1–6.

[11] L. U. Odhner, L. P. Jentoft, M. R. Claffee, N. Corson, Y. Tenzer, R. R. Ma, M. Buehler, R. Kohout, R. D. Howe, and A. M. Dollar, "A compliant, underactuated hand for robust manipulation," *The International Journal of Robotics Research*, vol. 33, no. 5, pp. 736–752, 2014.

[12] T. Taunyazov, L. S. Song, E. Lim, H. H. See, D. Lee, B. C. Tee, and H. Soh, "Extended tactile perception: Vibration sensing through tools and grasped objects," in *2021 IEEE/RSJ International Conference on Intelligent Robots and Systems (IROS)*. IEEE, 2021, pp. 1755–1762.

[13] A. W. Goodwin and H. E. Wheat, "Sensory signals in neural populations underlying tactile perception and manipulation," *Annu. Rev. Neurosci.*, vol. 27, pp. 53–77, 2004.

[14] K. Xu and N. Simaan, "An investigation of the intrinsic force sensing capabilities of continuum robots," *IEEE Transactions on Robotics*, vol. 24, no. 3, pp. 576–587, 2008.

[15] S. Zuo, J. Li, and M. Dong, "Design, modeling, and manipulability evaluation of a novel four-dof parallel gripper for dexterous in-hand manipulation," *Journal of Mechanical Science and Technology*, vol. 35, no. 7, pp. 3145–3160, 2021.

[16] F. Chen, F. Cannella, C. Canali, M. D'Imperio, T. Hauptman, G. Sofia, and D. Caldwell, "A study on data-driven in-hand twisting process using a novel dexterous robotic gripper for assembly automation," in *2014 IEEE/RSJ International Conference on Intelligent Robots and Systems*. IEEE, 2014, pp. 4470–4475.

[17] Robotiq, "The 2f series grippers," https://robotiq.com/products/2f85-140-adaptive-robot-gripper, 2022.

[18] F. Dimeas, D. V. Sako, V. C. Moulianitis, and N. A. Aspragathos, "Design and fuzzy control of a robotic gripper for efficient strawberry harvesting," *Robotica*, vol. 33, no. 5, pp. 1085–1098, 2015.

[19] J. Hashizume, T. M. Huh, S. A. Suresh, and M. R. Cutkosky, "Capacitive sensing for a gripper with gecko-inspired adhesive film," *IEEE Robotics and Automation Letters*, vol. 4, no. 2, pp. 677–683, 2019.

[20] S. Aoyagi, M. Suzuki, T. Morita, T. Takahashi, and H. Takise, "Bellows suction cup equipped with force sensing ability by direct coating thin-film resistor for vacuum type robotic hand," *IEEE/ASME Transactions on Mechatronics*, vol. 25, no. 5, pp. 2501–2512, 2020.

[21] Y. Yan, H. Wang, H. Yu, F. Wang, J. Fang, J. Niu, and S. Guo, "Machine learning-based surgical state perception and collaborative control for a vascular interventional robot," *IEEE Sensors Journal*, vol. 22, no. 7, pp. 7106–7118, 2022.

[22] W. Zhou, S. Guo, J. Guo, Z. Chen, and F. Meng, "Kinetics analysis and adrc-based controller for a string-driven vascular intervention surgical robotic system," *Micromachines*, vol. 13, no. 5, p. 770, 2022.

[23] X. Jin, S. Guo, J. Guo, P. Shi, M. Kawanishi, and H. Hirata, "Active suppression method of dangerous behaviors for robot-assisted vascular interventional surgery," *IEEE Transactions on Instrumentation and Measurement*, 2022.

[24] W. Zhou, S. Guo, J. Guo, F. Meng, Z. Chen, and C. Lyu, "A surgeon's habits-based novel master manipulator for the vascular interventional surgical master-slave robotic system," *IEEE Sensors Journal*, 2022.

[25] X. Li, S. Guo, P. Shi, X. Jin, and M. Kawanishi, "An endovascular catheterization robotic system using collaborative operation with magnetically controlled haptic force feedback," *Micromachines*, vol. 13, no. 4, p. 505, 2022.

[26] C. Yang, S. Guo, Y. Guo, and X. Bao, "Cloud communication-based sensing performance evaluation of a vascular interventional robot system," *IEEE Sensors Journal*, 2022.